# Increasing importance of regional emission controls for further reduction of $PM_{2.5}$ in Beijing

**Lingkai Dong[1,2], Weili Lin[3], Zhiqiang Ma[4], Wei Wang[5], Lei Kong[1,2], Xiaobin Xu[6], Oliver Wild[7], Yuanlin Wang[1,8,*], Baozhu Ge[1,2,*], Zifa Wang[1,2]**

[1]State Key Laboratory of Atmospheric Environment and Extreme Meteorology, Institute of Atmospheric Physics, Institute of Atmospheric Physics, Chinese Academy of Sciences, Beijing 100029, China

[2] University of Chinese Academy of Sciences, Beijing 100049, China

[3] College of Life and Environmental Sciences, Minzu University of China, Beijing 100081, China

[4] Institute of Urban Meteorology, China Meteorological Administration, Beijing, China

[5] National Center for Environmental Quality Forecast, China National Environmental Monitoring Centre, 100012, Beijing, China

[6] Key Laboratory for Atmospheric Chemistry, Chinese Academy of Meteorological Sciences, Beijing, China

[7] Lancaster Environment Centre, Lancaster University, Lancaster LA1 4YQ, United Kingdom

[8] UK Centre for Ecology & Hydrology, Bush Estate, Penicuik, Midlothian, EH26 0QB, United Kingdom

Submitted to *Urban Climate*

*Correspondence author:* Baozhu Ge (gebz@mail.iap.ac.cn) and Yuanlin Wang (yuawan@ceh.ac.uk)

# Abstract

Over the past decade, Beijing has achieved positive results in controlling fine particulate matter ($PM_{2.5}$) pollution. However, it remains a challenge to further reduce $PM_{2.5}$ concentrations to a lower level, such as the World Health Organization's air quality guidelines (5 μg/m$^3$). In this study, $PM_{2.5}$ concentrations and emission reductions over eight years covering two policy periods of air pollution abatement (2013–2017 and 2018–2020) were compared to investigate the efficiency of emission controls in Beijing and surrounding areas. An approach based on observational data, particularly including data from a regional atmospheric background station, was employed to calculate the relative contributions of the local emissions and regional transport. Results show that local emission reductions play a more important role in decreasing $PM_{2.5}$ in Beijing. However, following a substantial decrease in local emissions over the first period, the relative contribution of regionally transported $PM_{2.5}$ reached more than 50% during the second period. The results indicate that joint regional prevention and control of air pollution are needed for Beijing in the future. In addition, the background $PM_{2.5}$ concentrations over the North China Plain show an increasing trend in recent years, which may be attributed to the increased atmospheric oxidation capacity, thereby posing a challenge for further regional air quality management.



Keywords:

Regional transport, local emission, background level, relative contribution, air quality improvement, $PM_{2.5}$


Highlights:

1. The concentration and emission of $PM_{2.5}$ in Beijing showing a distinctive variation.
2. The regional joint control has great efficiency in reducing pollution.
3. After strictly limited, the $PM_{2.5}$ in Beijing became dominated by regional transport.
4. The $PM_{2.5}$ background level of North China Plain shown a significantly increasing.

# 1 Introduction

Fine particles with an aerodynamic equivalent diameter of 2.5 μm or less, known as $PM_{2.5}$, have been linked to numerous negative human health, including cardiovascular and pulmonary disease, as well as increased morbidity and mortality from respiratory and cardiovascular disease (Du et al., 2022; Liu et al., 2023; Sang et al., 2022; Seaton et al., 1995). Over the past two decades, China has experienced severe haze pollution, primarily caused by $PM_{2.5}$. This pollution is a result of rapid urbanization and industrialization (Xu et al., 2022; Zhu et al., 2023). The North China Plain (NCP) region, home to many of China's most polluted cities, experiences exacerbated pollution due to its topography and meteorological conditions (Li et al., 2023; Sun et al., 2017). To mitigate pollution, the state council of the People's Republic of China implemented a series of policies aimed at reducing air pollution. These include the Air Pollution Prevention and Control Action Plan (APPCAP) from 2013 to 2017 (Zhang et al., 2019b) and the Three-year Action Plan to Fight Air Pollution (TAPFAP) from 2018 to 2020 (Shao et al., 2023). As a result of these strict emission controls, Beijing has seen a significant decrease in annual average $PM_{2.5}$ concentrations, from 85 μg/m$^3$ in 2013 to 37 μg/m$^3$ in 2020. However, the concentration still far exceeds the World Health Organization's air quality guidelines (5 μg/m$^3$). Therefore, further efforts to mitigate $PM_{2.5}$ pollution remain a critical challenge for the future (Shu et al., 2023).

To address $PM_{2.5}$ pollution in the Beijing region, a crucial step is to quantify its sources. Anthropogenic emissions and meteorological conditions are widely recognized as the primary drivers of severe $PM_{2.5}$ pollution (Chen et al., 2020; Chen et al., 2025; Liu et al., 2021; Seinfeld et al., 1998; Wen et al., 2018). Regional transport also plays a significant role, particularly due to the surrounding industrial cities and unfavorable meteorological conditions (Feng et al., 2019; Li et al., 2021; Xu et al., 2023; Lin et al., 2008; Sun et al., 2023; Zhang et al., 2021b). Quantifying the influence in the neighboring region is necessary (Hernández-Moreno et al., 2023; Onishi et al., 2025).

Distinguishing the local emission contribution (LEC) and regional transport contribution (RTC) to pollution in Beijing is imperative for effective mitigation strategies. While short-term RTC during pollution events has been extensively studied using chemical transport models (Chen et al., 2019; Jiang et al., 2015; Li and Han, 2016; Lv et al., 2022; Wu et al., 2017; Zhang et al., 2019a; Zhang et al., 2021a; Zhang et al., 2021b), there remains a notable lack of research on the long-term impact of RTC across several years (Chen et al., 2021; Zhao et al., 2020). A key challenge in this area is the absence of accurate observational data to validate model predictions. Therefore, future research should focus on developing reliable measurement tools and long-term observational studies to better understand and quantify the RTC to $PM_{2.5}$ pollution in Beijing. This will be crucial for implementing effective regional prevention and control measures to reduce severe air pollution over the NCP (Lv et al., 2020; Xing et al., 2017).

Direct observations of the local and regional contributions to $PM_{2.5}$ are often challenging. To address this, Ge et al. (2018) developed an approach, based on observational data, to estimate the maximal regional transport contribution (MaxRTC) and the minimal local emission contribution (MinLEC) to air pollutants in Beijing. Subsequently, Tan et al. (2022) applied this method to analyze the trend in regional transport's contribution to $PM_{2.5}$ in Beijing during the APPCAP period, revealing a significant increase. In 2018, China introduced a new policy, TAPFAP, which imposed stricter emission limits on industries, motor vehicles, heating system, and other sources. Consequently, it has become essential to review and update our understanding of how regional transport contributes to $PM_{2.5}$ pollution in Beijing under these varying policies, in order to plan and implement effective pollution control measures in the future.

In this study, we employ the approach developed by Ge et al. (2018), incorporating an updated method for calculating the $PM_{2.5}$ background levels, to estimate the changes in the contributions of local emissions and regional transport to $PM_{2.5}$ in Beijing from 2013 to 2020. Our objective is to assess the effectiveness of the emission control measures implemented during the different policy periods. To achieve this, we have defined two phases: Phase I, spanning from 2013 to 2017and encompassing the APPCAP period; and Phase II, extending from 2015 to 2020 and covering the TAPFAP period, with targets referenced to 2015. The overall motivation was to provide new insights into future air pollution control strategies, aimed at achieving lower $PM_{2.5}$ concentrations.

# 2 Data and methods

## 2.1 Study area and measurement site descriptions

The NCP is the most populous plain in China, extending from the Yanshan Mountains in the north and Taihang Mountains in the west, and reaching Bohai Bay in the east (Figure 1(a)). The geography of the NCP is favorable for the formation of pollution episodes as the region is an air pollutant convergence zone. The westerly synoptic flow across the Taihang Mountains sinks and warms adiabatically, creating a low-pressure trough on the lee side (Jin et al., 2021b). During winter, the prevailing winds typically exhibit a northeasterly pattern, while during summer they shift to a southwesterly pattern, given the distinct influence of the subtropical high-pressure system (Fu et al., 2014; l., 2012; Jin et al., 2021a).

As Figure 2(a) shows, cities with high primary $PM_{2.5}$ emissions are located on the edge of the plain along the foothills of the mountains, and are distributed from southwest to northeast. Southwesterly transport occurs frequently during regional pollution episodes and serves as a trigger (Hu et al., 2022; Li et al., 2021). One of the most polluted cities is Shijiazhuang, in the southwest of the region, which is the capital of Hebei Province and often ranked as one of the most polluted cities in China. Beijing has relocated much of its industry to nearby regions, but still suffers from heavy pollution. Shangdianzi (SDZ) Station, situated northeast of Beijing within the Beijing municipality, is one of the regional Global Atmosphere Watch (GAW) stations in China, and it has only a few small villages and low anthropogenic emissions in its vicinity (Lin et al., 2008). Shijiazhuang was selected in this study as a typical polluted city to represent source regions on the NCP. Beijing was selected as the receptor area, while SDZ was selected as the background site to represent the background concentration of

$PM_{2.5}$ in the NCP region.

## 2.2 Observational data

The hourly $PM_{2.5}$, $SO_2$, $NO_2$ and CO concentration data from 2013 to 2020 at 87 sites in the NCP region were collected from the China National Environmental Monitoring Centre (CNEMC) (http://www.cnemc.cn, last access: 17 October 2024). Specifically, there are 12, 17 and 54 observation stations in Beijing, Tianjin and Hebei Province, respectively, including 9 stations in Shijiazhuang. To reduce errors from individual sites, the averaged $PM_{2.5}$ as well as the related pollutants (e.g., $SO_2$ and $NO_x$) concentrations from all stations within each city were calculated. The CNEMC observation network does not cover the background station. Therefore, data from the SDZ atmospheric background station in 2013–2020 operated by the China Meteorological Administration were used to represent the concentrations of pollutants in the BG region. Commercial instruments from Thermo Electron Corporation, USA, have been deployed to measure $O_3$ (TE 49C), NO/$NO_2$/$NO_x$ (TE 42ITL), CO (TE48C) and $SO_2$ (TE 43CTL) at SDZ. For $PM_{2.5}$, an R&P model TEOM 1400A instrument with a 2.5-µm cyclone inlet and a humidity control system was used. More details can be found in Zhao et al. (2009).

Emissions data for primary $PM_{2.5}$, $SO_2$ and $NO_x$ in the NCP region during the study period were obtained from the Multi-resolution Emissions Inventory for China (http://www.meicmodel.org, last access: 17 October 2024) (Li et al., 2017; Zheng et al., 2018), with a spatial resolution of 0.25° × 0.25°. The yearly averaged emissions of the three pollutants over the Beijing and Shijiazhuang areas during 2010–2020 were geographically averaged calculated, and these are listed in Table S1. Meteorological variables at Beijing and the SDZ background station during 2013–2020 were obtained from the China Meteorological Administration, and these were recorded at hourly resolution. The nearest site of meteorological measurement stations to the CNEMC stations were selected, with the distances between the meteorological and environmental stations not exceeding 500 meters.

## 2.3 Approach for distinguishing local emissions from regional transport

In this study, the relative contribution from local emissions and regional transport were calculated following the method of Ge et al. (2018). This approach has been widely used in other studies for the comparison with the model results in NCP (Yao et al., 2022; Khuzestani et al., 2022; Song et al., 2023; Qu et al., 2024), Shandong (Zhao et al., 2018) and Wuhan (Ma et al., 2021). The $PM_{2.5}$ concentrations in the background (B), receptor (R), and source (S) regions were divided into several parts:

$$C_S=C_{S\ local}+BK \tag{1}$$

$$C_R=C_{R\ local}+C_{Regional}+BK \tag{2}$$

$$C_B=\beta\cdot C_{R\ local}+C_{Regional}+BK \tag{3}$$

Here, $C_{local}$ represents the concentration contributed by local emissions, $C_{Regional}$ is the regional transport influences from polluted areas outside Beijing, which are mostly located to the south and east of Beijing. Figure 1 shows them at their respective sites. BK is the background concentration over the NCP, which is determined from clean air masses. $\beta$ reflect the relationship between local emissions ($C_{R\ local}$) in urban Beijing and the impacts on the SDZ background site, with the $\beta$ value always physically higher than zero. We assume that $C_{Regional}$ in receptor region R is the same as that in background region B based on the similar distance between the source region and the receptor and background regions. Indeed, the study by Ge et al. (2018) demonstrates that the uncertainty associated with this assumption can be ignored. Thus, the $C_{Regional}$ effects can be eliminated by subtracting Eq. (3) from Eq. (2), and then the MinLEC of urban Beijing can be calculated in Eq (4), and the MaxRTC can be deduced from Eq (5):

$$\text{Local}=\frac{C_{R\ local}}{C_R}=\frac{C_R\text{-}C_B}{(1\text{-}\beta)C_R}\geqslant\frac{C_R\text{-}C_B}{C_R} \tag{4}$$

$$\text{Transport}=\frac{C_{Regional}}{C_R}=\frac{C_R\text{-}BK\text{-}C_{R\ local}}{C_R}\leqslant\frac{C_B\text{-}BK}{C_R} \tag{5}$$

The difference between $C_R$ and $C_B$ is partly from the impacts of local emissions on the air pollutants in Beijing. A larger difference between $C_R$ and $C_B$ therefore corresponds to a larger MinLEC (Ge et al., 2018). Subtracting the BK value from $C_B$ represents the MaxRTC, since there are very limited local emissions in SDZ.

The background concentration BK in Eq. (5) is important in calculating MaxRTC and has usually been estimated based on the lowest concentration of air pollutants at the background station. Lin et al. (2009) picked the first peak in the frequency distribution of the concentration of air pollutants decomposed by two Lorentzian curve fittings as the background value. Ge et al. (2018) used this method to calculate the $PM_{2.5}$ in Beijing and SDZ, and took their average as BK value. However, the regional background is not constant over the long term. Changes can cause biases in calculating the contribution from regional transport using Eq. (5). Ruckstuhl et al. (2012) developed the Robust Extraction of Baseline Signal (REBS) technique to estimate the background level of trace gases and well-mixed air pollutants. This method is based on separation of pollutant concentration into three parts—the background value, regional contribution, and measurement errors from instruments—similar to the assumptions we use here, and has been applied at SDZ background station in other studies (Yao et al., 2012; Yao et al., 2014). However, Liu et al. (2019) argued that REBS was not suitable for estimating the background of carbon monoxide at SDZ, and instead recommended the meteorological method (MET) (Fang et al., 2014), which is based on the mean concentrations under specified meteorological conditions every year. To make our results more robust, both REBS and MET methods were employed in this study to estimate long-term $PM_{2.5}$ background concentrations over the NCP. More detailed descriptions of the mathematical functions and criteria used can be found in the supplementary materials.

To assess the effect of transport from the source region, the regional transport efficiency (α) was defined as

$$\alpha=\frac{C_{Regional}}{C_{S\ local}}\leqslant\frac{C_B\text{-BK}}{C_S\text{-BK}} \tag{6}$$

Following Eq. (1), $C_{S\ local}$ is the concentration in the source region after removal of background concentrations and represents the contribution that can be transported from the polluted areas. The ratio between $C_{S\ local}$ and $C_{Regional}$, given by $\alpha$, represents the efficiency of regional transport, with a higher value signifying a greater regional transport effect (RTE). Furthermore, to assess the efficiency of emission control on pollution mitigation, the emission control efficiency (ECE) proposed by Tan et al. (2022) was employed in this study. The ECE is expressed as the concentration change corresponding to given emission change of a certain air pollutant, and is calculated as the concentration decreasing rate (CDR) divided by the emission decreasing rate (EDR). More details can be found in supplementary materials.

# 3 Results and discussion

## 3.1 $PM_{2.5}$ changes under different policies

### 3.1.1 Significant mitigation of air pollution in Phase I

Figure 2 illustrates the spatiotemporal variation of observed $PM_{2.5}$ and associated primary emissions during the study period over the NCP region. In general, emissions in the NCP showed a significant decline in phase I, especially in the megacities of Shijiazhuang, Baoding, Tangshan, Beijing, and Tianjin, where the decrease exceeded 0.05 μg/m$^2$/s/yr. The decline in emissions in the surrounding rural areas is less pronounced. Table S2 lists the annual mean and maximum $PM_{2.5}$ concentrations for Beijing, the SDZ background station and Shijiazhuang. As expected, $PM_{2.5}$ concentrations in the NCP region showed a significant reduction in Phase I, associated with the implementation of emission controls. The largest reduction can be seen in Shijiazhuang, at approximately 20 μg/m$^3$/yr, which is twice or even three times the reduction seen in Beijing. However, the SDZ background station did not experience a significant change in concentration.

Table S1 summarizes the annual average emission rates, coal consumption, vehicle ownership, and GDP for Beijing and Shijiazhuang. Coal consumption has substantially reduced, while vehicle ownership and GDP have increased in both areas, particularly in Beijing. This suggests that most cities in the NCP region have reduced their emissions without compromising economic development. The emission control efficiencies for Beijing and Shijiazhuang are presented in Table 1. The value in Shijiazhuang is higher than that for Beijing, indicating that the source region (i.e., Shijiazhuang) has a higher control efficiency. Overemphasizing local emission control measures can make it more difficult and less efficient to abate air pollution, especially in a downstream receptor region such as Beijing (Tan et al., 2022).

### 3.1.2 Improvement slowdown in Phase II

In Policy II (TAPFAP), the government requires that the PM2.5 concentration in 2020 should be reduced by 18% compared to 2015. Therefore, for the analysis from a policy perspective, 2015 should be the target year for Phase II. As Figure 2(d) shows, the rate of emission reduction over the NCP in Phase II is slower. The rate of decline in primary $PM_{2.5}$ emissions in most industrial cities (e.g., Shijiazhuang, Baoding) is only about one fifth of that in Phase I, reaching 0.01–0.02 μg/m$^2$/s/yr. Tangshan experiences the largest reduction, at about 0.05 μg/m$^2$/s/yr. Similarly, the $PM_{2.5}$ concentration in most cities also shows a slower reduction, with the rate generally being below 10 μg/m$^3$/yr.

Taking Shijiazhuang as an example, the rate of reduction in $PM_{2.5}$ concentration during Phase II was −8.1 μg/m$^3$/yr (−10.8 μg/m$^3$/yr ($p < 0.01$) during 2018-2020), roughly half that in Phase I −17.3 μg/m$^3$/yr, see (Figure 3 a). This indicates that the change in $PM_{2.5}$ concentration aligns with the change in emissions in the source region. However, compared to Shijiazhuang, Beijing's emission reductions in Phase II were more significant, with major emission reductions rate in $PM_{2.5}$ and $SO_2$ (except $NO_x$) at about half that of Phase I (Figure 3 d). Interestingly, the rate of decline in the $PM_{2.5}$ concentration remains nearly constant from Phase II to Phase I (−8.7 μg/m$^3$/yr in Phase II (−7.4 μg/m$^3$/yr ($p < 0.01$) during 2018-2020) vs. −7.2 μg/m$^3$/yr in Phase I), which appears to contradict the decreasing rate of decline in precursor emissions in Beijing.

In contrast, the rest of the NCP region experiences a concurrent decrease in both the reduction rate of emissions and concentrations. Nevertheless, the rate of decrease in concentration in Beijing during Phase II is comparable to that in Shijiazhuang, and both are similar to other cities in the NCP region. Despite the slowdown in emissions reduction, the emission control efficiency in both Beijing and Shijiazhuang increases (Table 1), indicating more effective control of $PM_{2.5}$ emissions over the whole of the NCP in Phase II (Kong et al., 2023).

The results highlight controlling regional emissions is now more crucial for addressing pollution in Beijing than controlling local emissions, especially at low concentrations. This finding aligns with the model results of Lv et al. (2020), who simulated the effects of COVID-19 lockdown on reducing local traffic emissions in Beijing and their impacts on air quality. They found that although traffic emissions decreased substantially during the COVID-19 pandemic, their impacts on air quality were offset by the increased atmospheric oxidization capacity in surrounding regions. Consequently, they recommended synchronously controlling regional sources to maximize the benefits of controlling local traffic emissions.

## 3.2 Decreasing contribution of local emissions

In the past 10 years, numerous studies have focused on the relative contributions to air pollution in Beijing from local emissions and regional transport. A total of 30 publications that discuss the regional transport and the local emission contributions to $PM_{2.5}$ pollution in Beijing during 2013–2020 are reviewed here. The sources, methods and key findings are summarized in Table S3. Most of these studies focused on single case studies, with only five simulated the annual average contribution. None of them accounted for the variation from year to year. Additionally, most previous studies quantified the contribution using a chemical transport model, leaving a gap for reliable assessments based on observations.

In this study, an approach based on observations was employed to estimate the MinLEC and MaxRTC to $PM_{2.5}$ in Beijing. Figure 4 (a) presents the results for MinLEC in Beijing between 2013 and 2020. The citations of these studies can be found in the supplementary materials. The results of the MinLEC to $PM_{2.5}$ in Beijing are within the range of previously reported literature values, with consistent temporal variation from 2013-2019. Specifically, during the first three years, the MinLEC displayed a slightly increasing trend from 53% in 2013 to 58% in 2015. The median values of various models during different periods show a significant increase from 46% in 2013 to 61% in 2015. However, starting from 2015, it shows a significant decrease, dropping to nearly 30% by 2019. An independent samples t-test was conducted to compare the differences between the periods of 2013-2015 and 2018-2020. The results revealed a statistically significant difference between the mean value of the two groups, with a t-value of -8.96 ($p < 0.01$). These findings suggest that the reduction in local emissions is likely the dominant factor contributing to Beijing's $PM_{2.5}$ mitigation efforts. The decline in local emissions may have led to a reduction of 30.7 μg/m$^3$ in $PM_{2.5}$ concentrations over the last eight years and could be the primary reason why the concentration in Beijing has declined at a rate similar to that of other cities.

Our values for MinLEC fall within the range of LEC values reported in the literature, but are slightly lower. This difference is likely due to our calculation providing an estimate of the lower limit of LEC. The difference between MinLEC and the LEC derived from other studies highlights the need for further validation of the impact of the rapid decrease in local emissions.

## 3.3 Increasing contribution of regional transport

As shown in Figure 4 (b), the MaxRTC in Beijing experienced a significant increase, rising from 40% in 2013 to nearly 50% in 2020. Regional transport is significantly affected by the wind direction, particularly when southerly winds dominate (Hu et al., 2022; Li et al., 2021). Yang et al. (2016) assessed the frequency of southerly winds using the sine of the vector-average wind direction and found that it contributed 22% to $PM_{2.5}$ pollution in Beijing. Despite successful emission control measures in surrounding cities, where $C_{s\ local}$ has shown a substantial decline (Figure 5 a), their relative impacts on Beijing's air quality are intensifying. The differences between $C_{s\ local}$ and $C_{Regional}$ are narrowing, indicating the increased importance of regional transport (Figure 5 a). It is worth noting that RTE exhibited a strong seasonal variation, indicating that meteorological conditions, rather than the $C_{s\ local}$, are the main factor instead driving the trend. The regional transport effect depicted in Figure 5(b) displays a significant increasing trend of 2.2% $yr^{-1}$. Concurrently, the sine of the vector-average wind direction showed the opposite trend, further indicating a potential relationship between southerly winds and the regional contribution to $PM_{2.5}$ in Beijing.

As mentioned above, the $PM_{2.5}$ concentration across the entire NCP region decreased significantly due to the emission control measures. However, the yearly background values, calculated using REBS method, show an increase from 7.25 $\mu g/m^3$ in 2013 to more than 10 $\mu g/m^3$ after 2016 (Table S2). This increase is also confirmed by the results obtained from the MET method, as shown in Figure 5 (c, d). In contrast to previous studies (Ge et al., 2018; Tan et al., 2022), background values have been increasing year by year, suggesting they may play an increasingly important role in the variation of $PM_{2.5}$ pollution over the NCP region, particularly during future clean-up periods when $PM_{2.5}$ concentrations reach very low levels. Besides, the nighttime $PM_{2.5}$ and nighttime $O_3$ during the high $O_3$ concentrations periods show a positive correlation with R reached at 0.39 ($p<0.01$, two-tailed significance). On the contrary, negative correlation was found during low $O_3$ concentrations periods (-0.26, $p < 0.01$). This suggests that increases in nighttime ozone concentrations tend to coincide with increases in nighttime PM2.5 from 2013 to 2020, which may be due to the dominance of secondary sources for both nighttime ozone and $PM_{2.5}$. Furthermore, it is also worth noting that incorporating the background contribution into the regional effect (MaxRTC + Background) increases the RTC estimate for the 2019-2020 period to 70%, which is close to the median value reported in other studies. This evidence highlights the importance of considering the background as an important factor, as it can substantially influence estimates of the contribution of regional transport (up to 30% in this study).

## 3.4 Enhanced background value

As mentioned above, the background level of $PM_{2.5}$ at the SDZ station showed a clear upward trend during 2013-2020 (Figure 5 d). This trend is also evidenced by the concentration heatmap at the SDZ background station (Figure S2), which demonstrates a notable increase in low concentration values. The Hybrid Single Particle Lagrangian Integrated Trajectory (HYSPLIT) model was employed to generate 72-hour air masses backward trajectories from 2013 to 2020. The GDAS meteorological datasets with horizontal resolution of 0.5° from the Air Resources Laboratory (ARL) were used. These backward trajectories start from the SDZ background station at 100 m height AGL (Figure 6 a-h)), with a restart every 6 h. They were calculated and clustered annually to enhance the representativeness of the trajectory ensembles. As shown in Table S4 and Figure 6 (i, j), the averaged concentrations of $PM_{2.5}$ and $O_3$ were calculated for each cluster. Although the air masses clusters varied from year to year, three typical clusters were evident at the SDZ stations, one characterized by southbound short-range and two by northbound short- and long-range. It is worth noting that both of the $PM_{2.5}$ and $O_3$ concentrations from north direction showed a significant increasing trend with more frequency, especially in long-range clusters. This could be one of the reasons for the increasing background level of $PM_{2.5}$ in NCP region.

In order to investigate in-depth, yearly variations in different percentiles (5%, 25%, 50%, 75%, 95%) of $PM_{2.5}$ and $O_3$ concentrations from 2013 to 2020 were calculated and shown in Figure 7a (selected percentiles) and Figure S3 (whole dataset). The significant reduction in $PM_{2.5}$ concentrations above the $75^{th}$ percentile is attributable to the pollution controls implemented in the NCP region in recent years. In contrast, a slight upward trend in $PM_{2.5}$ concentrations below the $25^{th}$ percentile is considered to indicate an increase in background levels. The nighttime $O_3$ concentrations also displayed a clear upward trend, especially at the $95^{th}$ percentile. In order to explore the relationship between low concentration of $PM_{2.5}$ and nighttime $O_3$, wind rose were plotted (Figure 7 b and c). The results show a clear similarity in wind direction and wind frequency distribution, with high values originating from the northwest. In other words, the increase in low $PM_{2.5}$ concentrations from the northwest is associated with an increase in higher nighttime $O_3$ concentrations. Besides, the nighttime $PM_{2.5}$ and nighttime $O_3$ during the high $O_3$ concentrations periods show the positive correlation with coefficient reached at 0.39 ($p<0.01$, two-tailed significance). On the contrary, negative correlation was found during low $O_3$ concentrations periods (-0.26, $p<0.01$). This suggests that elevated nighttime $O_3$ concentrations tend to coincide with the increased nighttime $PM_{2.5}$ from 2013 to 2020. These may be due to the fact that higher $O_3$ concentrations at nighttime enhance the oxidative production of secondary aerosols. At night, $O_3$ oxidizes $NO_2$ to form $NO_3$ radicals, which subsequently react with $NO_2$ to form $N_2O_5$ (Brown and Stutz, 2012), thus leading to the formation of secondary aerosols through heterogeneous chemistry (Jo et al., 2019; Qu et al., 2019).

# 4 Implications and conclusions

In this study, we compared two phases of $PM_{2.5}$ pollution variations in the NCP region from 2013 to 2020 and found that Phase I exhibited more substantial emission reductions across most NCP cities compared to Phase II. Figure 8 illustrates the evolving contributions of local emissions and regional transport across the two policy periods. MinLEC exhibits a decreasing trend, while MaxRTC demonstrates an upward trend. A comparison of the median values between the two policy periods reveals a significant shift, with MinLEC decreasing by 18% and MaxRTC increasing by 7%. Furthermore, the relative contribution of regional transport to $PM_{2.5}$ pollution in Beijing has increased notably. To effectively address future $PM_{2.5}$ pollution in Beijing, it is imperative to consider the influence of the surrounding areas from a broader, regional perspective.

Despite the observation-based approach in this study, which does not account for all $PM_{2.5}$ dynamics, our findings highlight a notable increase in regional contributions. Additionally, $PM_{2.5}$ background concentrations in the NCP region have risen in recent years, surpassing the World Health Organization's air quality guidelines. Achieving further reductions in $PM_{2.5}$ pollution will require long-term, large-scale control measures. Policymakers should address not only primary emissions from urban and industrial areas but also broader meteorological and atmospheric oxidant factors. Such an approach is vital to meet China's pollution and carbon reduction targets over the next decade.

# ASSOCIATED CONTENT

## Supporting Information

Detailed Information about the REBS and MET methods, along with supporting tables and figures, is provided in the supporting information.

## Data availability

The data that support the findings of this study are available on request from the corresponding author, Prof. Ge, upon reasonable request.

# AUTHOR INFORMATION

## Corresponding Author

*Phone: +86-10-62063256. E-mail: gebz@mail.iap.ac.cn and yuawan@ceh.ac.uk.

## Notes

The authors declare no competing financial interests.

## Author statement

**Lingkai Dong:** Methodology, Formal analysis, Data Curation, Writing - Original Draft, Visualization. **Weili Lin:** Investigation, Data Curation. **Zhiqiang Ma:** Investigation, Data Curation. **Wei Wang:** Investigation, Data Curation. **Lei Kong:** Investigation, Data Curation. **Xiaobin Xu:**

Resources, Data Curation. **Oliver Wild:** Validation, Writing - Review & Editing. **Yuanlin Wang:** Data Curation, Funding acquisition, Writing – review & editing. **Baozhu Ge:** Conceptualization, Writing - Review & Editing, Supervision, Funding acquisition. **Zifa Wang:** Supervision, Project administration.

# ACKNOWLEDGMENTS

We are grateful to CNEMC for providing the observation data over the NCP. This work was financially supported by the National Natural Science Foundation of China (Grants 42122049 and 42377104), the National Key Research and Development Program of China (Grant No. 2022YFC3702002) and the CAS Strategic Priority Research Program (Grant No. XDB0760403).

# REFERENCES


Brown, S.S., Stutz, J., 2012. Nighttime radical observations and chemistry. Chem. Soc. Rev. 41. https://doi.org/10.1039/c2cs35181a.

Chen, L., Zhu, J., Liao, H., Gao, Y., Qiu, Y., Zhang, M., Liu, Z., Li, N., Wang, Y., 2019. Assessing the formation and evolution mechanisms of severe haze pollution in the Beijing–Tianjin–Hebei region using process analysis. Atmos. Chem. Phys. 19, 10845–10864. https://doi.org/10.5194/acp-19-10845-2019.

Chen, Z., Chen, D., Zhao, C., Kwan, M.P., Cai, J., Zhuang, Y., Zhao, B., Wang, X., Chen, B., Yang, J., Li, R., He, B., Gao, B., Wang, K., Xu, B., 2020. Influence of meteorological conditions on PM2.5 concentrations across China: a review of methodology and mechanism. Environ. Int. 139, 105558. https://doi.org/10.1016/j. envint.2020.105558.

Chen, D., Xia, L., Guo, X., Lang, J., Zhou, Y., Wei, L., Fu, X., 2021. Impact of inter-annual meteorological variation from 2001 to 2015 on the contribution of regional transport to PM2.5 in Beijing, China. Atmos. Environ. 260. https://doi.org/10.1016/j.atmosenv.2021.118545.

Chen, G., Han, Y., Wang, X., Zhang, Y., Liu, Y., Dong, L., Zhou, Q., Xiao, P., 2025. Interaction influence characteristics of air quality and aerosol properties between Beijing-Tianjing-Hebei (BTH) and Yangtze River Delta (YRD), China. Urban Clim. 61. https://doi.org/10.1016/j.uclim.2025.102395.

Du, H., Liu, Y., Shi, G., Wang, F., He, M.Z., Li, T., 2022. Associations between source-specific fine particulate matter and mortality and hospital admissions in Beijing, China. Environ. Sci. Technol. 56, 1174–1182. https://doi.org/10.1021/acs.est.1c07290.

Fang, S.X., Zhou, L.X., Tans, P.P., Ciais, P., Steinbacher, M., Xu, L., Luan, T., 2014. In situ measurement of atmospheric CO2 at the four WMO/GAW stations in China. Atmos. Chem. Phys. 14, 2541–2554. https://doi.org/10.5194/acp-14-2541-2014.

Feng, T., Zhou, W., Wu, S., Niu, Z., Cheng, P., Xiong, X., Li, G., 2019. High-resolution simulation of wintertime fossil fuel CO2 in Beijing, China: characteristics, sources, and regional transport. Atmos. Environ. 198, 226–235. https://doi.org/10.1016/j.atmosenv.2018.10.054.

Fu, G.Q., Xu, W.Y., Yang, R.F., Li, J.B., Zhao, C.S., 2014. The distribution and trends of fog and haze in the North China plain over the past 30 years. Atmos. Chem. Phys. 14, 11949–11958. https://doi.org/10.5194/acp-14-11949-2014.

Ge, B., Wang, Z., Lin, W., Xu, X., Li, J., Ji, D., Ma, Z., 2018. Air pollution over the North China plain and its implication of regional transport: a new sight from the observed evidences. Environ. Pollut. 234, 29–38. https://doi.org/10.1016/j.envpol.2017.10.084.

Hern´andez-Moreno, A., Trujillo-P´aez, F.I., Mugica-´Alvarez, V., 2023. Quantification of primary PM2.5 mass exchange in three Mexican megalopolis metropolitan areas. Urban Clim. 51. https://doi.org/10.1016/j.uclim.2023.101608.

Hu, Q., Liu, C., Li, Q., Liu, T., Ji, X., Zhu, Y., Xing, C., Liu, H., Tan, W., Gao, M., 2022. Vertical profiles of the transport fluxes of aerosol and its precursors between Beijing and its southwest cities. Environ. Pollut. 312, 119988. https://doi.org/10.1016/j.envpol.2022.119988.

Jiang, C., Wang, H., Zhao, T., Li, T., Che, H., 2015. Modeling study of PM2.5 pollutant transport across cities in China's Jing–Jin–Ji region during a severe haze episode in December 2013. Atmos. Chem. Phys. 15, 5803–5814. https://doi.org/10.5194/acp-15-5803-2015.

Jin, X., Cai, X., Huang, Q., Wang, X., Song, Y., Zhu, T., 2021a. Atmospheric boundary layer—free troposphere air exchange in the North China plain and its impact on PM2.5 pollution. J. Geophys. Res. Atmos. 126, e2021JD034641. https://doi.org/10.1029/2021JD034641.

Jin, X., Cai, X., Yu, M., Wang, X., Song, Y., Kang, L., Zhang, H., Zhu, T., 2021b. Mesoscale structure of the atmospheric boundary layer and its impact on regional air pollution: a case study. Atmos. Environ. 258. https://doi.org/10.1016/j.atmosenv.2021.118511.

Jo, H.-Y., Lee, H.-J., Jo, Y.-J., Lee, J.-J., Ban, S., Lee, J.-J., Chang, L.-S., Heo, G., Kim, C.-H., 2019. Nocturnal fine particulate nitrate formation by N2O5 heterogeneous chemistry in Seoul metropolitan area, Korea. Atmos. Res. 225, 58–69. https://doi.org/10.1016/j.atmosres.2019.03.028.

Khuzestani, R.B., Liao, K., Liu, Y., Miao, R., Zheng, Y., Cheng, X., Jia, T., Li, X., Chen, S., Huang, G., Chen, Q., 2022. Spatial variability of air pollutants in a megacity characterized by mobile measurements. Atmos. Chem. Phys. 22, 7389–7404. https://doi.org/10.5194/acp-22-7389-2022.

Kong, L., Tang, X., Wang, Z., Zhu, J., Li, J., Wu, H., Wu, Q., Chen, H., Zhu, L., Wang, W., Liu, B., Wang, Q., Chen, D., Pan, Y., Li, J., Wu, L., Carmichael, G.R., 2023. Changes in air pollutant emissions in China during two clean-air action periods derived from the newly developed inversed emission inventory for Chinese air quality (CAQIEI). Earth Syst. Sci. Data Discussions 2023, 1–47. https://doi.org/10.5194/essd-2023-477.

Li, J., Han, Z., 2016. A modeling study of severe winter haze events in Beijing and its neighboring regions. Atmos. Res. 170, 87–97. https://doi.org/10.1016/j. atmosres.2015.11.009.

Li, M., Liu, H., Geng, G., Hong, C., Liu, F., Song, Y., Tong, D., Zheng, B., Cui, H., Man, H., Zhang, Q., He, K., 2017. Anthropogenic emission inventories in China: a review. Natl. Sci. Rev. 4, 834–866. https://doi.org/10.1093/nsr/nwx150.

Li, J., Gao, W., Cao, L., He, L., Zhang, X., Yan, Y., Mao, J., Xin, J., Wang, L., Tang, G., Liu, Z., Ji, D., Hu, B., Zhao, D., Zhao, S., Jia, D., Wang, Y., 2021. Effects of different stagnant meteorological conditions on aerosol chemistry and regional transport changes in Beijing, China. Atmos. Environ. 258. https://doi.org/ 10.1016/j.atmosenv.2021.118483.

Li, Y., Gao, Q., Gao, W., Du, W., Hu, X., Zhang, K., 2023. Meteorological factors related to winter severe PM2.5 pollution in China: in perspective of thresholds and relation of occurrence frequency with east Asian trough. Atmospheric. Pollut. Res. 15, 102002. https://doi.org/10.1016/j.apr.2023.102002.

Lin, W., Xu, X., Zhang, X., Tang, J., 2008. Contributions of pollutants from North China plain to surface ozone at the Shangdianzi GAW Station. Atmos. Chem. Phys. 8, 5889–5898. https://doi.org/10.5194/acp-8-5889-2008.

Lin, W., Xu, X., Ge, B., Zhang, X., 2009. Characteristics of gaseous pollutants at Gucheng, a rural site southwest of Beijing. J. Geophys. Res.-Atmos. 114, D00g14, 17. https://doi.org/10.1029/2008jd010339.

Liu, S., Fang, S., Liang, M., Ma, Q., Feng, Z., 2019. Study on CO data filtering approaches based on observations at two background stations in China. Sci. Total Environ. 691, 675–684. https://doi.org/10.1016/j.scitotenv.2019.07.162.

Liu, J., Chu, B., Chen, T., Zhong, C., Liu, C., Ma, Q., Ma, J., Zhang, P., He, H., 2021. Secondary organic aerosol formation potential from ambient air in Beijing: effects of atmospheric oxidation capacity at different pollution levels. Environ. Sci. Technol. 55, 4565–4572. https://doi.org/10.1021/acs.est.1c00890.

Liu, M., Lei, Y., Wang, X., Xue, W., Zhang, W., Jiang, H., Wang, J., Bi, J., 2023. Source contributions to PM2.5-related mortality and costs: evidence for emission allocation and compensation strategies in China. Environ. Sci. Technol. 57, 4720–4731. https://doi.org/10.1021/acs.est.2c08306.

Lv, Z., Wang, X., Deng, F., Ying, Q., Archibald, A.T., Jones, R.L., Ding, Y., Cheng, Y., Fu, M., Liu, Y., Man, H., Xue, Z., He, K., Hao, J., Liu, H., 2020. Source–receptor relationship revealed by the halted traffic and aggravated haze in Beijing during the COVID-19 Lockdown. Environ. Sci. Technol. 54, 15660–15670. https://doi. org/10.1021/acs.est.0c04941.

Lv, L., Wei, P., Hu, J., Chen, Y., Shi, Y., 2022. Source apportionment and regional transport of PM2.5 during haze episodes in Beijing combined with multiple models. Atmos. Res. 266. https://doi.org/10.1016/j.atmosres.2021.105957.

Ma, Y., Zhu, Y., Liu, B., Li, H., Jin, S., Zhang, Y., Fan, R., Gong, W., 2021. Estimation of the vertical distribution of particle matter (PM2.5) concentration and its transport flux from lidar measurements based on machine learning algorithms. Atmos. Chem. Phys. 21, 17003–17016. https://doi.org/10.5194/acp-21-17003-2021.

Onishi, K., Yumimoto, K., Okuda, T., Fukuike, A., Maki, T., Nojima, M., Shinoda, M., Nakayama, T., Kurozawa, Y., Yamagata, Z., Kurosaki, Y., 2025. Transboundary air pollution in coastal urban area in Japan: transport model and positive matrix factorization analysis for SPM-PM2.5 and PM2.5. Urban Clim. 59. https://doi.org/ 10.1016/j.uclim.2024.102237.

Qu, Y., Chen, Y., Liu, X., Zhang, J., Guo, Y., An, J., 2019. Seasonal effects of additional HONO sources and the heterogeneous reactions of N2O5 on nitrate in the North China plain. Sci. Total Environ. 690, 97–107. https://doi.org/10.1016/j.scitotenv.2019.06.436.

Qu, K., Yan, Y., Wang, X., Jin, X., Vrekoussis, M., Kanakidou, M., Brasseur, G.P., Lin, T., Xiao, T., Cai, X., Zeng, L., Zhang, Y., 2024. The effect of cross-regional transport on ozone and particulate matter pollution in China: a review of methodology and current knowledge. Sci. Total Environ. 947, 174196. https://doi.org/ 10.1016/j.scitotenv.2024.174196.

Ruckstuhl, A.F., Henne, S., Reimann, S., Steinbacher, M., Vollmer, M.K., O'Doherty, S., Buchmann, B., Hueglin, C., 2012. Robust extraction of baseline signal of atmospheric trace species using local regression. Atmos. Meas. Tech. 5, 2613–2624. https://doi.org/10.5194/amt-5-2613-2012.

Sang, S., Chu, C., Zhang, T., Chen, H., Yang, X., 2022. The global burden of disease attributable to ambient fine particulate matter in 204 countries and territories, 1990-2019: a systematic analysis of the global burden of disease study 2019. Ecotoxicol. Environ. Saf. 238, 113588. https://doi.org/10.1016/j. ecoenv.2022.113588.

Seaton, MacNee, W., Donaldson, K., Godden, D., 1995. Particulate air pollution and acute health effects. Lancet 345, 177–178. https://doi.org/10.1016/S0140-6736 (95)90173-6.

Seinfeld, J.H., Pandis, S.N., Noone, K., 1998. Atmospheric chemistry and physics:

from air pollution to climate change. Phys. Today 51, 88–90. https://doi.org/10.1063/1.882420.

Shao, T., Wang, P., Yu, W., Gao, Y., Zhu, S., Zhang, Y., Hu, D., Zhang, B., Zhang, H., 2023. Drivers of alleviated PM2.5 and O3 concentrations in China from 2013 to 2020. Resour. Conserv. Recycl. 197, 107110. https://doi.org/10.1016/j.resconrec.2023.107110.

Shu, Y., Li, H., Wagner, F., Zhang, S., Yang, T., Klimont, Z., Kiesewetter, G., Wang, H., Sander, R., Binh, N., 2023. Pathways toward PM2.5 air quality attainment and its CO2 mitigation co-benefits in China's northern cities by 2030. Urban Clim. 50. https://doi.org/10.1016/j.uclim.2023.101584.

Song, Y., Xing, C., Liu, C., Lin, J., Wu, H., Liu, T., Lin, H., Zhang, C., Tan, W., Ji, X., Liu, H., Li, Q., 2023. Evaluation of transport processes over North China plain and Yangtze River Delta using MAX-DOAS observations. Atmos. Chem. Phys. 23, 1803–1824. https://doi.org/10.5194/acp-23-1803-2023.

Sun, J., Huang, L., Liao, H., Li, J., Hu, J., 2017. Impacts of regional transport on particulate matter pollution in China: a review of methods and results. Curr. Pollut. Rep. 3, 182–191. https://doi.org/10.1007/s40726-017-0065-5.

Sun, T., Zhang, T., Xiang, Y., Fan, G., Fu, Y., Lv, L., 2023. Investigation on the vertical distribution and transportation of PM2.5 in the Beijing-Tianjin-Hebei region based on stereoscopic observation network. Atmos. Environ. 294. https://doi.org/10.1016/j.atmosenv.2022.119511.

Tan, Q., Ge, B., Xu, X., Gan, L., Yang, W., Chen, X., Pan, X., Wang, W., Li, J., Wang, Z., 2022. Increasing impacts of the relative contributions of regional transport on air pollution in Beijing: observational evidence. Environ. Pollut. 292, 118407. https://doi.org/10.1016/j.envpol.2021.118407.

Wen, W., He, X., Ma, X., Wei, P., Cheng, S., Wang, X., Liu, L., 2018. Understanding the regional transport contributions of primary and secondary PM2.5 components over Beijing during a severe pollution episodes. Aerosol Air Qual. Res. 18, 1720–1733. https://doi.org/10.4209/aaqr.2017.10.0406.

Wu, J., Li, G., Cao, J., Bei, N., Wang, Y., Feng, T., Huang, R., Liu, S., Zhang, Q., Tie, X., 2017. Contributions of trans-boundary transport to summertime air quality in Beijing, China. Atmos. Chem. Phys. 17, 2035–2051. https://doi.org/10.5194/acp-17-2035-2017.

Xing, J., Wang, S., Zhao, B., Wu, W., Ding, D., Jang, C., Zhu, Y., Chang, X., Wang, J., Zhang, F., Hao, J., 2017. Quantifying nonlinear multiregional contributions to ozone and fine particles using an updated response surface modeling technique. Environ. Sci. Technol. 51, 11788–11798. https://doi.org/10.1021/acs.est.7b01975.

Xu, W., Yao, L., Fu, X., Wang, Y., Sun, S., 2022. Response of PM2.5 variations to changing urbanization process in different climatic backgrounds of China. Urban Clim. 45. https://doi.org/10.1016/j.uclim.2022.101273.

Xu, J., Lu, M., Guo, Y., Zhang, L., Chen, Y., Liu, Z., Zhou, M., Lin, W., Pu, W., Ma, Z., Song, Y., Pan, Y., Liu, L., Ji, D., 2023. Summertime urban ammonia emissions may be substantially underestimated in Beijing, China. Environ. Sci. Technol. 57, 13124–13135. https://doi.org/10.1021/acs.est.3c05266.

Yang, Y., Liao, H., Lou, S., 2016. Increase in winter haze over eastern China in recent decades: roles of variations in meteorological parameters and anthropogenic emissions. J. Geophys. Res. Atmos. 121. https://doi.org/10.1002/2016jd025136.

Yao, B., Vollmer, M.K., Xia, L., Zhou, L., Simmonds, P.G., Stordal, F., Maione, M., Reimann, S., O'Doherty, S., 2012. A study of four-year HCFC-22 and HCFC-

142b in- situ measurements at the Shangdianzi regional background station in China. Atmos. Environ. 63, 43–49. https://doi.org/10.1016/j.atmosenv.2012.09.011.

Yao, B., Zhou, L., Xia, L., Zhang, G., Guo, L., Liu, Z., Fang, S., 2014. Atmospheric sulfur hexafluoride in-situ measurements at the Shangdianzi regional background station in China. J. Environ. Sci. (China) 26, 2451–2458. https://doi.org/10.1016/j.jes.2014.03.004.

Yao, S., Zhang, H., Wang, Q., 2022. Vertical distribution of PM2.5 transport flux in summer and autumn in Beijing. Aerosol Air Qual. Res. 22. https://doi.org/10.4209/ aaqr.220143.

Zhang, H., Cheng, S., Yao, S., Wang, X., Zhang, J., 2019a. Multiple perspectives for modeling regional PM2.5 transport across cities in the Beijing–Tianjin–Hebei region during haze episodes. Atmos. Environ. 212, 22–35. https://doi.org/10.1016/j.atmosenv.2019.05.031.

Zhang, Q., Zheng, Y., Tong, D., Shao, M., Wang, S., Zhang, Y., Xu, X., Wang, J., He, H., Liu, W., Ding, Y., Lei, Y., Li, J., Wang, Z., Zhang, X., Wang, Y., Cheng, J., Liu, Y., Shi, Q., Yan, L., Geng, G., Hong, C., Li, M., Liu, F., Zheng, B., Cao, J., Ding, A., Gao, J., Fu, Q., Huo, J., Liu, B., Liu, Z., Yang, F., He, K., Hao, J., 2019b. Drivers of improved PM2.5 air quality in China from 2013 to 2017. Proc. Natl. Acad. Sci. USA 116, 24463–24469. https://doi.org/10.1073/pnas.1907956116.

Zhang, W., Hai, S., Zhao, Y., Sheng, L., Zhou, Y., Wang, W., Li, W., 2021a. Numerical modeling of regional transport of PM2.5 during a severe pollution event in the Beijing–Tianjin–Hebei region in November 2015. Atmos. Environ. 254, 118393. https://doi.org/10.1016/j.atmosenv.2021.118393.

Zhang, Y., Chen, X., Yu, S., Wang, L., Li, Z., Li, M., Liu, W., Li, P., Rosenfeld, D., Seinfeld, J.H., 2021b. City-level air quality improvement in the Beijing-Tianjin-Hebei region from 2016/17 to 2017/18 heating seasons: attributions and process analysis. Environ. Pollut. 274, 116523. https://doi.org/10.1016/j. envpol.2021.116523.

Zhao, X., Zhang, X., Xu, X., Xu, J., Meng, W., Pu, W., 2009. Seasonal and diurnal variations of ambient PM2.5 concentration in urban and rural environments in Beijing. Atmos. Environ. 43, 2893–2900. https://doi.org/10.1016/j.atmosenv.2009.03.009.

Zhao, X., Gao, Q., Sun, M., Xue, Y., Ma, R., Xiao, X., Ai, B., 2018. Statistical analysis of spatiotemporal heterogeneity of the distribution of air quality and dominant air pollutants and the effect factors in Qingdao urban zones. Atmosphere 9. https://doi.org/10.3390/atmos9040135.

Zhao, N., Wang, G., Li, G., Lang, J., Zhang, H., 2020. Air pollution episodes during the COVID-19 outbreak in the Beijing-Tianjin-Hebei region of China: An insight into the transport pathways and source distribution. Environ. Pollut. 267, 115617. https://doi.org/10.1016/j.envpol.2020.115617.

Zheng, B., Tong, D., Li, M., Liu, F., Hong, C., Geng, G., Li, H., Li, X., Peng, L., Qi, J., Yan, L., Zhang, Y., Zhao, H., Zheng, Y., He, K., Zhang, Q., 2018. Trends in China's anthropogenic emissions since 2010 as the consequence of clean air actions. Atmos. Chem. Phys. 18, 14095–14111. https://doi.org/10.5194/acp-18-14095-2018.

Zhu, T., Liu, X., Wang, X., He, H., 2023. Technical development and prospect for collaborative reduction of pollution and carbon emissions from iron and steel industry in China. Engineering. https://doi.org/10.1016/j.eng.2023.02.014.

# Tables

Table 1 The concentration decrease rate (CDR), emission decrease rate (EDR), and emission control efficiency (ECE) of $PM_{2.5}$ in Beijing and Shijiazhuang during the different policy periods.

| Index | Phase I | | Phase II [a] | |
|---|---|---|---|---|
| | Beijing | Shijiazhuang | Beijing | Shijiazhuang |
| CDR (%) | −9.9 | −13.7 | −15.1 | −8.2 |
| EDR (%) | −11.1 | −12.0 | −11.3 | −5.5 |
| EDR [b] (%) | −6.9 | −12.9 | −2.9 | −4.8 |
| ECE | 0.89 | 1.14 | 1.31 | 1.48 |
| ECE [b] | 1.44 | 1.06 | 5.22 | 1.71 |

a: To avoid the influence of COVID-19, the averages for 2015 and 2019 were chosen for calculation.
b: Emissions contain primary $PM_{2.5}$, $SO_2$ and $NO_x$.

# Figures

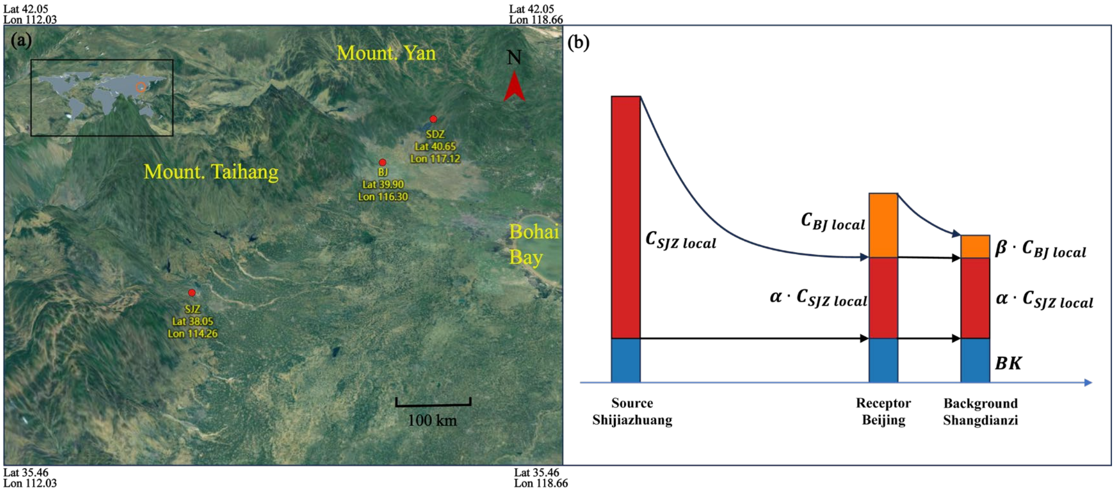


**Figure 1.** (a) Geographic locations and terrain of the NCP and the three cities/stations in this study— Shijiazhuang (SJZ), Beijing (BJ), and Shangdianzi (SDZ) (source: NASA satellite map; http://worldwind.arc.nasa.gov). (b) Assumptions regarding $PM_{2.5}$ concentrations in the three regions.

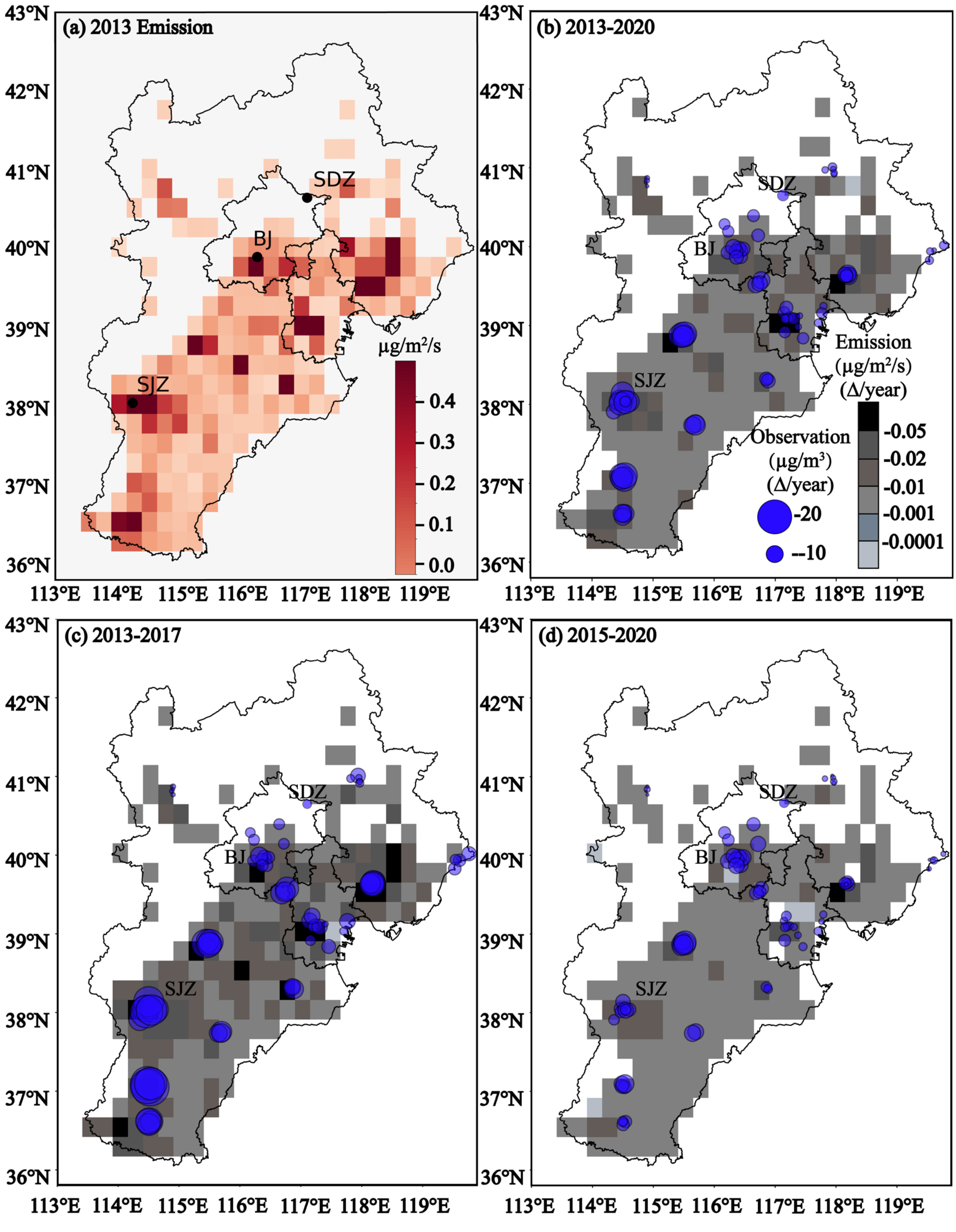


**Figure 2.** Spatial distribution of (a) NCP emissions in 2013, and (b–d) reductions in emissions (shading) and concentrations at observation sites (spots) during (b) 2013–2020, (c) 2013–2017, and (d) 2015–2020. Grid points with emissions below 0.02 μg/m$^2$/s are ignored.

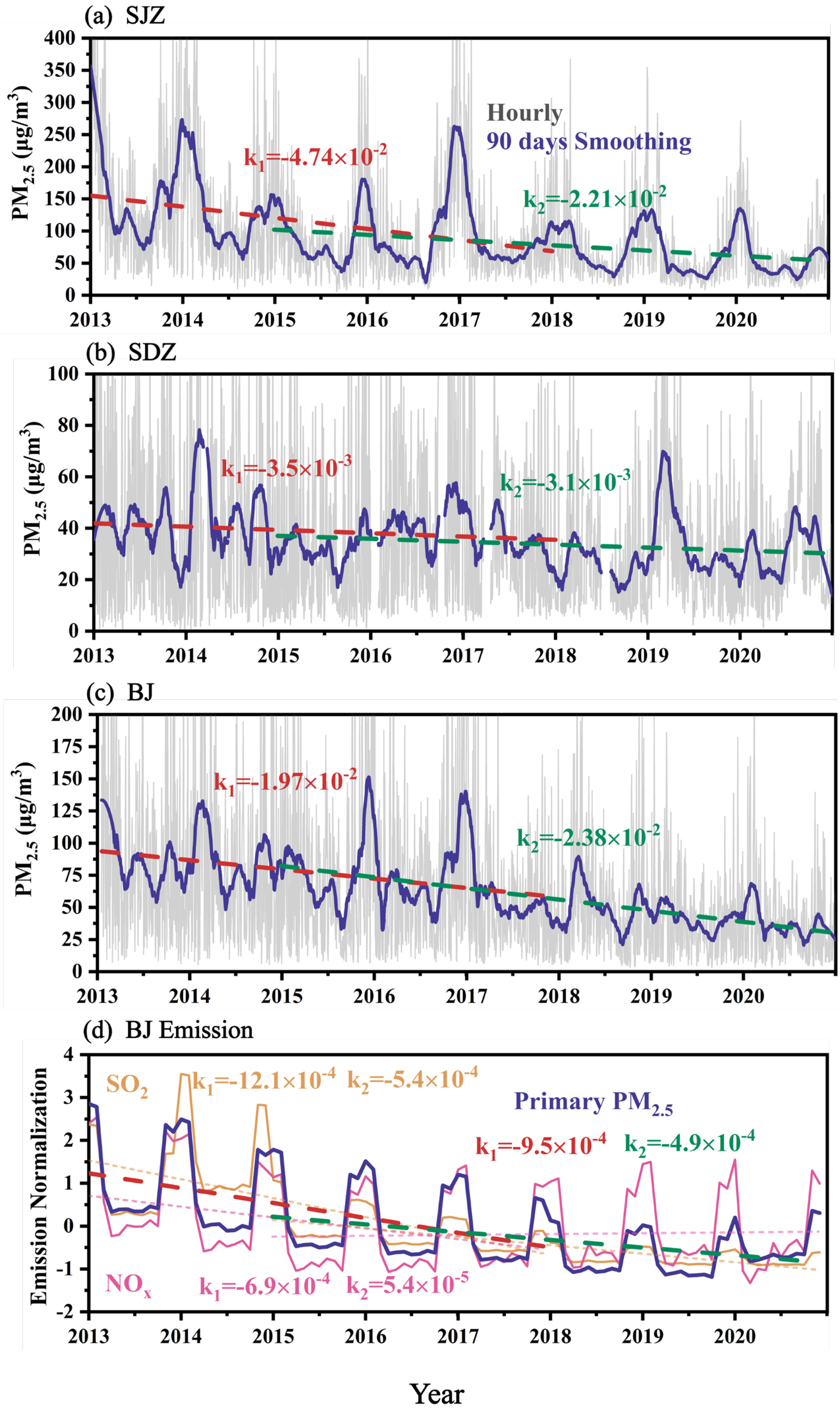


**Figure 3**. Time series of the concentration for site (a) SJZ, (b) SDZ, (c) BJ and (d) Normalized emissions of primary $PM_{2.5}$, $SO_2$ and $NO_x$ from 2013 to 2020. The 90 days smoothed curves (blue), and the linear regression lines during Phase I (red dashed line), and Phase II (green dashed line) were also plotted. The slope ($k_1$, $k_2$) units are μg/m$^3$/d in (a-c) and μg/m$^2$/s/m in (d).

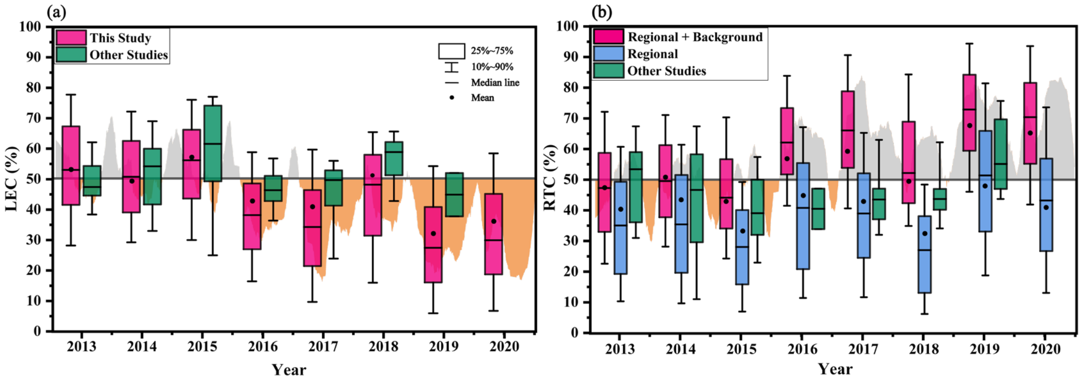


**Figure 4.** Box plots of the (a) local emissions contribution (LEC) and (b) regional transport contribution (RTC) calculated in this study and other studies (references summarized in Table S3). The black lines mark contribution = 50%. Gray ang orange shading indicate the contribution of more than 50% and less than 50%, respectively.

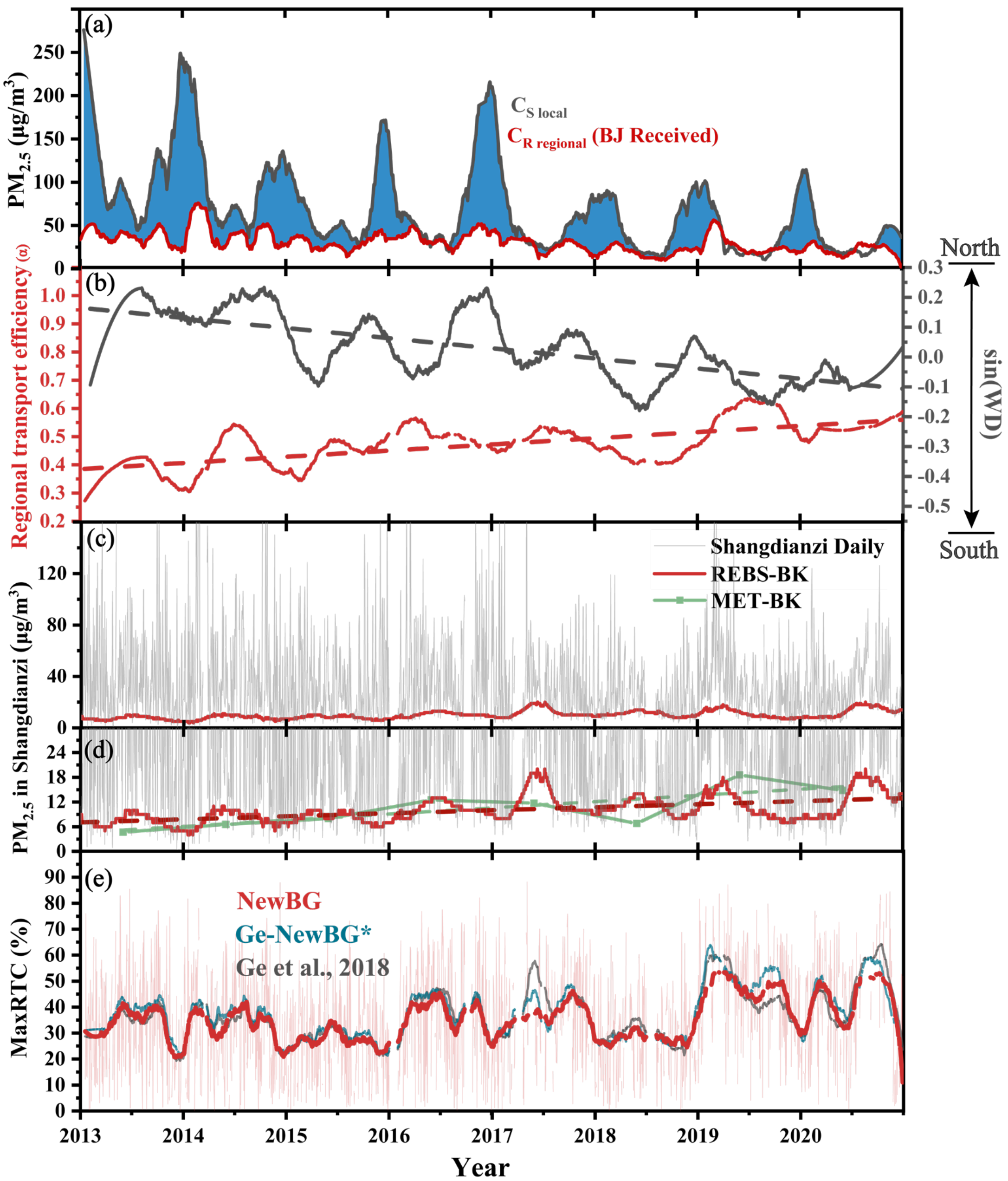


**Figure 5.** (a) Local $PM_{2.5}$ concentrations in Shijiazhuang and regional pollution transport received in Beijing, and (b) trends of regional transport effeciency α and the sin(WD), and (c, d) the time series of $PM_{2.5}$ daily mean concentration in Shangdianzi (grey) and the background values calculated by the REBS method (red) and the MET method (green), and (e) variations in MaxRTC under three different background level: background values calculated from Ge et al. (2018) method (black), using Beijing and Shangdianzi averages (blue), and using REBS (red).

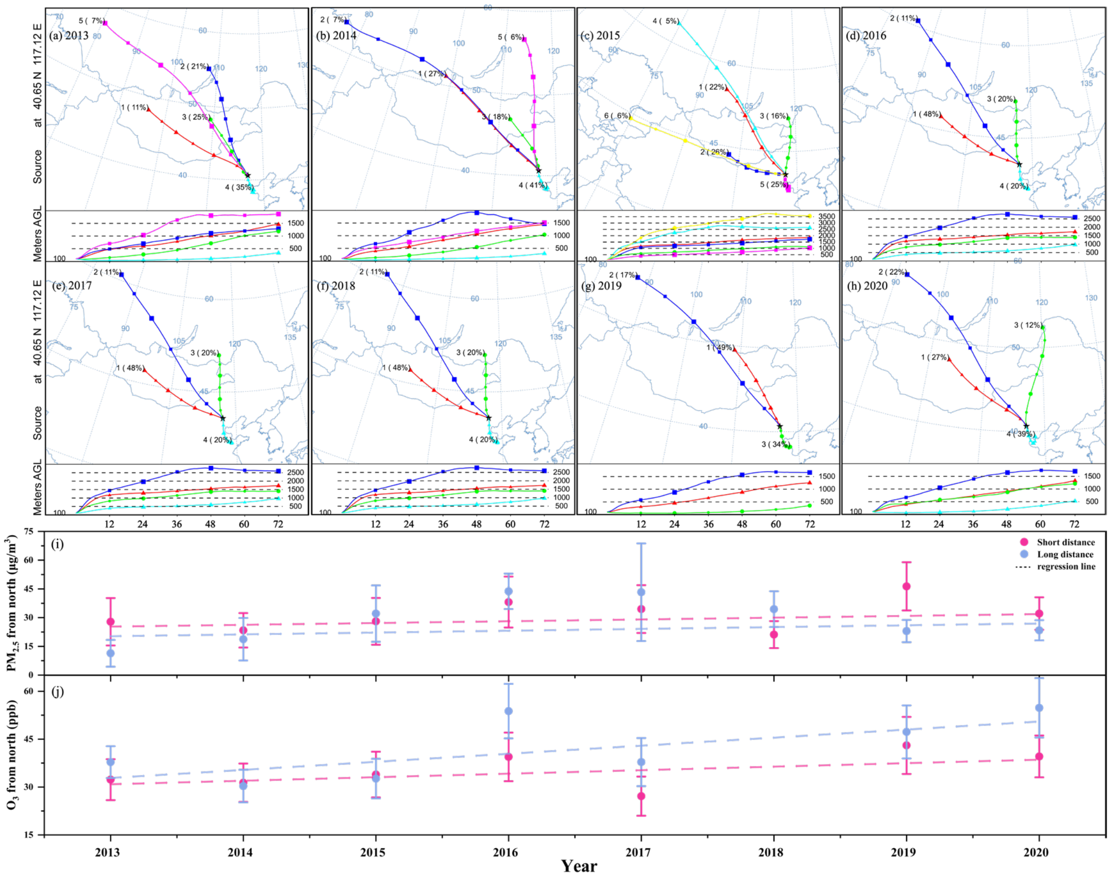


**Figure 6.** The 72-hour backward traectories over the Shangdianzi station for each year from 2013 to 2020 (a-h), respectively. The annual average concentration of $PM_{2.5}$ (i) and $O_3$ (j) in the north trajectories from 2013 to 2020.

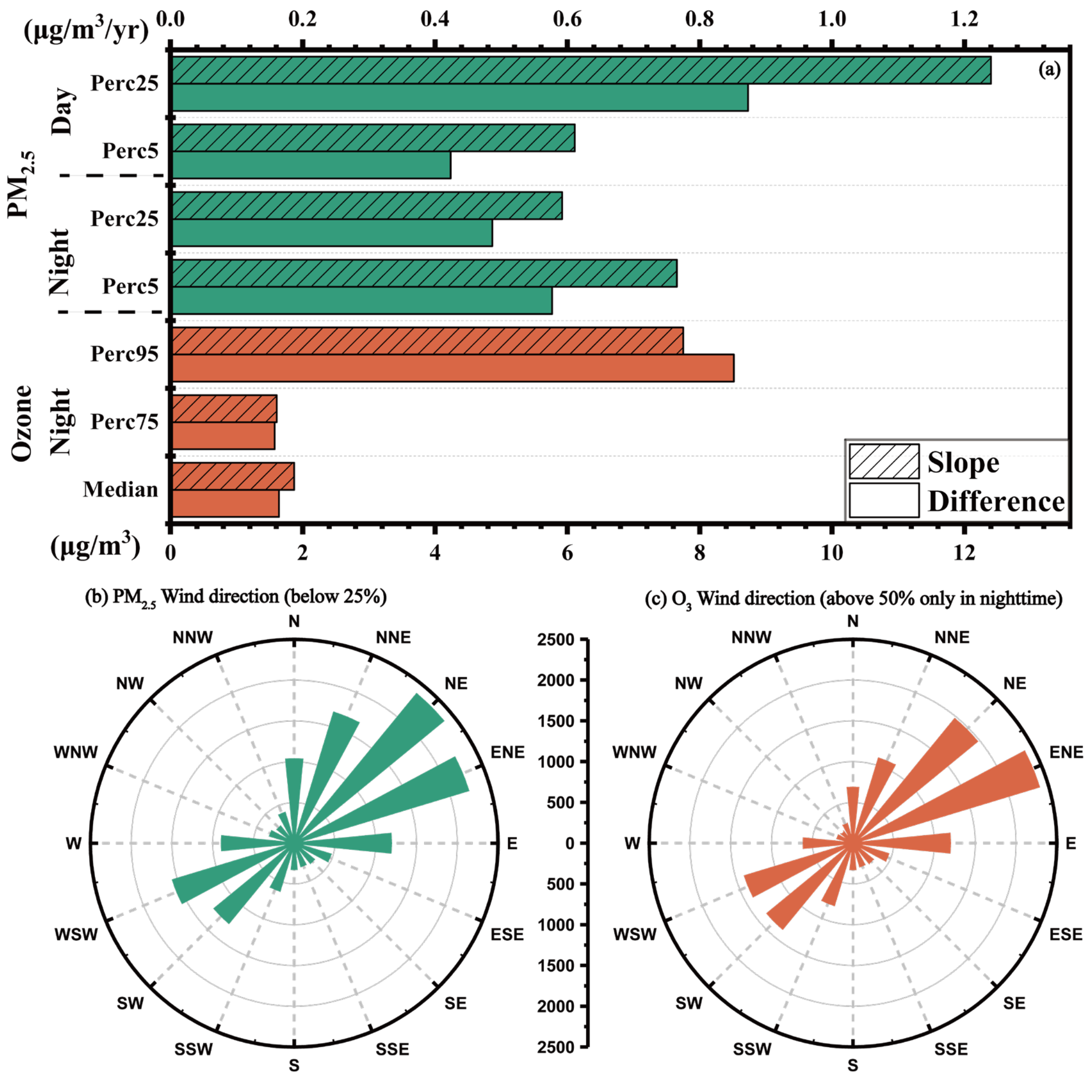


**Figure 7.** Changes in different percentiles of $PM_{2.5}$ and $O_3$ between 2013 and 2020 (a), Wind rose plots for the lowest 25% of $PM_{2.5}$ (b) and the highest 50-100% of nighttime $O_3$ (c). The abbrevations of Per5, Per25, Median, Per75 and Per95 at the vertical coordinate of figure (a) represent 5, 25, 50, 75 and 95 percentile, respectively.

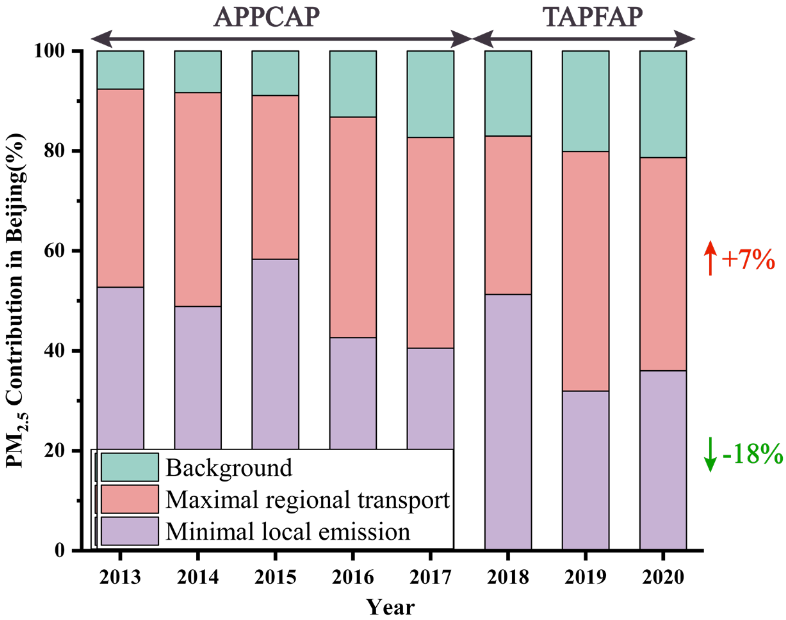


**Figure 8.** Annual changes in the MinLEC, MaxRTC and background values of $PM_{2.5}$ levels in Beijing, along with their median changes between the two policy periods.